International Atomic Energy Agency

INDC(NDS)-153/L

INDC INTERNATIONAL NUCLEAR DATA COMMITTEE

A SURVEY OF NEUTRON ENERGY SPECTRA AND ANGULAR DISTRIBUTIONS OF THE $^{9}BE(p,n)^{9}B$ REACTION FOR FAST NEUTRON RADIOTHERAPY

Malika ALLAB
Nuclear Data Section
International Atomic Energy Agency

March 1984

IAEA NUCLEAR DATA SECTION, WAGRAMERSTRASSE 5, A-1400 VIENNA

INDC(NDS)-153/L

A SURVEY OF NEUTRON ENERGY SPECTRA AND ANGULAR DISTRIBUTIONS OF THE $^{9}BE(p,n)^{9}B$ REACTION FOR FAST NEUTRON RADIOTHERAPY

Malika ALLAB
Nuclear Data Section
International Atomic Energy Agency

March 1984

A Survey of Neutron Energy Spectra and Angular Distributions of the $^{9}Be(p,n)^{9}B$ Reaction for Fast Neutron Radiotherapy

Malika ALLAB *
Nuclear Data Section
International Atomic Energy Agency

Abstract

Encouraging findings in radiobiology have stimulated a renewed use of fast neutrons in radiotherapy. The physical characteristics required for neutron beams to be suitable for radiotherapy are well established. As a result, the tendency is to replace the previous machines which generated the neutron beams from deuteron bombardment of thick targets (T, Li, Be) by hospital based cyclotrons which accelerate protons on thick Beryllium targets. This report, suggested by Dr. K. OKAMOTO from the IAEA Nuclear Data Section, surveys the available experimental data of the $^{9}Be(p,n)$ reaction (cross sections, neutron spectra, yields, mean neutron energies) from the threshold to the proton energy E_p = 120 MeV and the works using this reaction in dosimetry measurements, with an emphasis on the data since 1977.

Introduction

Soon after the discovery of the neutron, the application of fast neutrons to radiotherapy started with the 37 inch cyclotron at Berkeley in the U.S.A.. After nearly 30 years interruption, because of partly severe late effects observed in the normal tissues of many patients, the neutron radiotherapy was recently brought back to the stage, as a consequence of recent findings leading to a better understanding of radiobiological effects.

* on leave from the Université des Sciences et de la Technologie "Houari Boumedienne", Algiers, Algeria.

The reason for the use of fast neutrons in radiotherapy is first to overcome the so called "oxygen effect". This term describes the observation that hypoxic cells, contained in the centre of most solid tumors, show greater resistance to radiation than well-oxygenated cells, contained in most normal tissues; this resistance is much smaller for neutrons than for conventional radiation such as X-rays. Furthermore, the phenomenon of repair of sublethal damage after irradiation is weaker for neutrons than for X-rays and this could have, in some cases, in fractionated radiotherapy, clinical advantages. The last point arguing for the use of fast neutrons is the result of investigations on the radiosensitivity of cells in different cell cycle stages, with the conclusion that the variation of this radiosensitivity is less for neutrons than for X-rays; consequently a higher Relative Biological Effectiveness can be achieved for some tumors and less variation in response from tumor to tumor will be observed after neutron than after X-ray irradiation (see BR81 and references therein).

Up to now, the majority of clinical trials of neutron therapy has been performed with cyclotrons or neutron generators constructed for other purposes generally unsuitable for radiotherapy. The encouraging results have led to assess the main characteristics of a neutron beam and its source suitable for therapy. Extensive surveys by Cross (CR77, CR78) outline the data requirements both for interpreting the clinical trials and for the construction of new accelerators. The reactions considered by Cross as neutron sources are induced by deuteron or proton beams on thick lithium or beryllium targets.

So far, the cyclotron-produced neutron beams for radiotherapy were generally generated by deuterons on thick beryllium targets; but, as modern cyclotrons can produce protons with energies twice as high as the deuteron energies, there is a trend towards using proton beams. Therefore, the data of the Be(p,n) reaction have been thoroughly surveyed, following Cross' work, with an emphasis on new experimental results since 1977.

Neutron beams from the proton bombardment of beryllium targets are being implemented for current use in radiotherapy (JO78, AL79, BR82, HA82, SM82, AW83, HA83, ME83). Hence, a great interest has developed in

facilities providing neutron beams of sufficient high flux and suitable energy that could optimize the required clinical beam-specifications such as a high dose rate (> 20 rad/min) at a satisfactory target to skin distance (TSD ~ 125 cm), an acceptable penetration depth for 50% of maximum dose (~ 13.2 cm), a flattened dose distribution, and others.

Various physical properties of the neutron beams, particularly the dose build-up, and the dose along and perperdicular to the central beam axis, beam collimation, and shielding designs depend on the energy spectra and angular distributions of the neutrons. Therefore, a number of experiments has been conducted in which angular distributions, spectra shapes and neutron absolute yields have been determined for proton energies up to 120 MeV with both thin and thick targets and different target backings; a survey of the available data is presented in Table 1. At these energies, the neutrons are chiefly obtained from the $^{9}Be(p,n)^{9}B$ reaction (Q = -1.85 MeV) but three body break-up reactions can also give rise to a large component of low energy neutrons:

$^{9}Be\ (p,n\alpha)^{5}Li$ (Q = -3,54 MeV)
$^{9}Be\ (p,pn)^{8}Be$ (Q = -1,67 MeV)
$^{9}Be\ (p,\alpha p)^{5}He$ (Q = -2,67 MeV)
$\longrightarrow \alpha + n$ (Q = +0.89 MeV)

1) The angular distributions

At low proton energies, the neutrons from the ^{9}Be (p,n) reaction are associated to the ^{9}B ground state, the contributions of the excited states (2,3 MeV...) growing more and more as the proton energy E_p increases (fig.1). Cross section measurements for the different neutron groups have been performed using thin targets. Their angular distributions, shown in fig. 1, exhibit, at forward angles, clearly defined peaks that become sharper with increasing proton energy. The same trend can also be observed in the angular distributions of total neutron yields measured with thick beryllium targets by Kuchnir et al. (KU73), Lone et al. (LO77) and Johnsen et al. (JO77), displayed in fig. 2. However, great discrepancies exist between the absolute values of the neutron yields given by the two latter authors at E_p = 23 MeV and 25 MeV

respectively; Johnson's values at 0^{o} are nearly four times lower than Lone's values, probably because of the high neutron threshold (5 MeV) compared to the 0.3 MeV fixed in Lone's experiments. This suggests a high portion of low energy neutrons not suitable for radiotherapy, particularly when a tumor is deep-seated, because such lower energy neutrons are preferentially absorbed in the skin, thus having a high RBE (Relative Biological Effectiveness) at the surface.

2) The neutron energy spectra

As the neutron yields are largest at forward angles, most of the neutron energy spectra have been measured at a neutron detection angle $\theta=0^{o}$.

Till now, the most systematic studies of the neutron energy spectra have been performed by the UCRL Davis Laboratory in a proton energy range 25 MeV $\leqslant E_p \leqslant$ 65 MeV (JO77, AM77, HE77, JO78), using thick beryllium targets with several thicknesses, 0.46 cm $\leqslant T_t \leqslant$ 3.25 cm, and in some cases, spectrum hardening polyethylene filters of various thicknesses.

For 30 MeV $\leqslant E_p \leqslant$ 40 MeV, these spectra show a large low energy component of evaporation neutrons, together with a higher energy component which peaks near 20 MeV (JO78) and slowly decreases beyond the kinematic limit because of the energy resolution which, at high energies, is limited by the short flight paths fixed in the time-of-flight measurements. However, a significant discrepancy has been observed in the shape of these spectra and in the magnitude of the neutron yields measured at Davis and those measured later elsewhere by Waterman et al. (WA79) at E_p=35 MeV and 46 MeV and by Graves et al. (GR79) at E_p=41 MeV. This discrepancy has recently been resolved by the Davis Group who performed new measurements of the E_p=35 MeV neutron spectrum using a thinner target, just stopping the proton beam, and, for neutron detection, a proton recoil spectrometer instead of the time-of-flight technique (UL81). The corrected spectrum is in good agreement in shape with Grave's, Waterman's and Turco's results (GR79, WA79, TU80):

especially, at neutron energies above 10 MeV, it is more flat than that previously reported. In magnitude, the agreement is also fairly good, as confirmed by the integral neutron yield which is 16.6 x 10^9 neutrons/sr/μC in the Davis group measurements and 16.3 x 10^9 neutrons/sr/μC as deduced from Waterman's data. Furthermore, the high energy portion of the latest Davis Group spectrum, measured by using the proton recoil technique is better defined. The more reliable 0^o neutron energy spectra in the energy region around E_p = 40 MeV are displayed in fig. 3.

At lower energies ($E_p \sim 25$ MeV), the spectra measured by Lone et al. (LO77) at 23 MeV and by Johnsen et al. (JO77) at 25 MeV present nearly the same shape as that described above, as can be seen in fig. 3; however, the constant high energy part is more slowly decreasing up to the kinematic limit. Furthermore, a noticeable discrepancy exist in the absolute values of the 23 and 25 MeV neutron yield measurements that might be covered partly by the experimental uncertainties not clearly estimated by the authors.

At higher energies ($E_p \gtrsim 60$ MeV), no experimental information exists on the low energy part of the neutron spectra. The available data (see Table 1) performed with time of flight techniques show a high threshold fixed by the longest flight time limited by the overlapping of successive proton beam bursts. The measurements at 65 MeV (AM77) and at 100 MeV (MA77, HA80) performed with targets, that stop completely or partly the 65 MeV or the 100 MeV proton beam respectively, show a pronounced peak at a neutron energy in the range $0.35\ E_p \leqslant E_n \leqslant 0.45\ E_p$; however, at 65 MeV, this peak is progressively reduced when thinner targets are used and disappears completely exhibiting a nearly constant yield when the incident beam loses by ionisation only half of its energy (fig. 4). It must be noticed that these 65 MeV measurements, performed by Davis Laboratory and published nearly at the same time as the earlier 35 MeV spectrum, have to be considered cautiously; for no other spectrum data allowing comparisons are reported at this energy. Nevertheless, many dosimetry measurements and treatment planning procedures induced by such a beam are already in progress at Fermilab (AW80, AW81, RO81, AW82, AW83, TE83) and at Louvain-la-Neuve (ME83, VY83). At E_p = 100 MeV, the shapes of the existing spectra measured with different neutron detection

techniques (MA77, HA80) are in fairly good agreement (fig. 4) but no absolute evaluation of the neutron yield has been made.

3) Neutron yields and average energies

The neutron yields and average energies depend on the target thickness, filtration and cut-off energy of the neutron beams.

Some 0^{o} integral yields and average energies, selected between E_p = 12 MeV and E_p = 100 MeV are displayed in Table 2. As can be seen, the lowest experimental neutron thresholds reached are E_{th} = 0.4 MeV at $E_p \simeq$ 20 MeV (LO81) and E_{th} = 1 MeV at E_p = 40 MeV (WA79), and the actual shape and therefore the neutron yields at very low energies are still unknown. Several extrapolation procedures have been proposed: a linear falloff, leading to a vanishing neutron yield at zero energy (JO77), a linear or exponential extrapolation to the zero neutron energy (GR79, WA79); more recently, the low energy tail of the spectrum has been approximated by an evaporation distribution (AW83), which depends on the experimental parameters such as, for instance, the beam filtration. Therefore, the 0 MeV threshold yields and average energies, given in the literature and reported in the Table 2, are somewhat doubtful. On the other hand, the 2 MeV threshold 0^{o} neutron yields I_n and the average energies $\bar{E}_n$ deduced by Lone et al. (LO81) from lower threshold energy measurements are more certain. They have been estimated by the following empirical expressions that give a satisfactory fit to the experimental data in the energy range 10 MeV < E_p < 50 MeV:

$$\bar{E}_n = 0.47\ E_p - 2.2 \qquad \text{(energies in MeV)}$$

$$I_n = 1.6\ E_p^{2.2} \cdot 10^{13} \qquad \text{(n/sr/C)},$$

pointing out increasing $\bar{E}_n$ and I_n values as E_p increases, I_n being in good agreement with the relative dose per unit incident charge proposed earlier by Awschalom et al. (AW80b):

$$D(E_p) \propto E_p^{\beta} \qquad \text{with } 2.2 \leqslant \beta \leqslant 3.2$$

Nevertheless, the contribution of the low energy neutrons, undesirable in radiotherapy because of their lower effective penetration, can be reduced either by introducing hydrogeneous filters into the beam line, as shown in figure 5, or by the use of thinner targets to reduce the degradation of the proton beam energy in the target, responsible for a large part of these low energy neutrons. Both methods improve the penetration of the beam by hardening the average energy $\bar{E}_n$ but reduce to some extent the neutron yield (Table 2) and therefore the dose rate.

4) Target design and filtration

Several dosimetric measurements have been performed recently to investigate the improvement of the clinical neutron beam by either or both of the two above mentioned methods. Some general conclusions are drawn below.

Thus, inserting a 6 cm thick nylon filter in a E_p = 42 MeV p + Be neutron beam increases the depth of the 50% neutron dose in a water phantom from 12 cm to 13.5 cm (MI78). Furthermore, the effects of polythene filters added on a thick beryllium target (T_t = 3.8 cm, sufficient to stop 80 MeV protons) subjected to 30 - 75 MeV protons have shown that five centimeters of polythene increase the penetration of the neutron beam in water to about the same extent as an increase of 15 MeV in proton energy (fig. 6). However, the loss of dose rate amounts to a factor of about 2 for a filter of about 6-10 cm thickness, as estimated from the different absolute experimental measurements reported by Bewley et al. (BE80) and from other data in relative units (GR78, SM82).

A combination of the two methods, namely filtration of semithick targets neutron beams, has been thoroughly checked by Rosenberg et al. (RO81a) and by Smathers et al. (SM82) and thus a higher penetration could be achieved with less of a reduction in dose rate (fig. 7).

Rosenberg et al. (RO81a) have derived from experimental measurements some empirical algebraic expressions connecting the depth for half maximum dose $Z(e_t,o)$ and the maximum dose per unit current $D(e_t,o)$ from the unfiltered targets removing the energy e_t from the incident energy E_p:

$$\frac{D(e_t,0)}{D(E_p,0)} = 1-\left[\frac{1}{a}\left(\frac{Z(e_t,0)}{Z(E_p,0)}-1\right)\right]^{\beta/b}$$

whereas, after filtration by polyethylene filters of various thicknesses, the same quantities (Ze_t, filt) and $D(e_t$, filt) are connected by:

$$\frac{Z(e_t,filt)}{Z(e_t,0)} = 1 + m\left[1-\frac{D(e_t,filt)}{D(e_t,0)}\right]$$

The constants a,b,β and m have been deduced from the experimental data at E_p = 42 MeV.

Therefore, for a clinically desired dose rate, the use of such transmission targets requires higher beam currents involving high target power dissipation and beryllium heating problems. The accepted safe limits are about 2.5 - 3.2 kW/cm^2 to guarantee a long life of water cooled Be targets (AW80a). To allow a judicious choice of the target, Awschalom et al. (AW80a) have compared the properties of a 45 MeV proton beam on Be targets of various thicknesses, namely on the one hand the relative beam current required to maintain a constant dose rate and the corresponding beam power dissipation in the targets, and on the other hand, at constant power dissipation in the targets, the relative beam currents tolerated and the consequent relative dose rates.

Several considerations suggested that beryllium targets should be "thin", i.e. they should not remove the whole proton energy; the residual proton energy has to be dissipated in backstop materials characterized by a high thermal conductivity and a low neutron and γ production. Tantalum, copper or carbon backings are generally used. But it has been shown that thick copper backstop leads to discrepancies from expected behaviour either in entrance dose or penetration depth or relative dose measurements as progressively thinner targets are used (AW80b) because the backstop contribution is more and more significant and approaches that of a pure copper target as evaluated by Smathers et al. (SM82). This suggests that very thin beryllium targets are impractical.

Several target designs have recently been evaluated to optimize the clinical quality of the neutron beam (RO81a, SM82, TO82, ME83, VY83).

For instance at E_p = 41 MeV, it was concluded (SM82) that the desired depth dose and dose rate at a satisfactory TSD are achieved with a significant reduction in beryllium heating problems if a copper backed target removing 70% from the incident proton beam is used with 5-6 cm polyethylene filters. However, using 1.59 mm of copper to absorb the transmitted beam (SM82) or a 0.25 mm of copper followed by 1.3 mm of water and 8 mm of pyrolytic graphite (R081a) does not effect the depth in phantom at which the 50% of maximum dose occurs. At E_p = 65 MeV, the target assembly producing a neutron therapy beam consists of 17.3 mm of beryllium removing 34.8 MeV (53%) of the proton energy, backed with 8.5 mm of carbon and followed by a 2 cm polyethylene filter (VY83, ME83); carbon backing is preferred to brass backing because of its larger negative Q value (Q = -18,1 MeV) and its lower γ production: indeed, the residual activation measured after four hours of therapy treatment with the above described target in beam axis is, at patient position, 800 mRem/h, four times lower than that measured with a 10 mm Be target backed with 7 mm brass equal to 2500 mRem/h, unacceptable for patient safety. A further improvement of the ambient activity is obtained by inserting the target in a movable support to remove it away from the beam axis.

Besides the dosimetric measurements necessary to characterize the neutron beams, the radiobiological effects have also to be taken into account. Several authors have studied the dependence of the oxygen enhancement ratio (OER) and/or the RBE on the neutron energy (HA76, VA81, HA82a and references indicated therein). However, as the main question arising from the use in radiotherapy of neutrons generated by proton bombardment of thick beryllium targets is the higher RBE at the surface than at depth, Hall et al. (HA82, HA83) have investigated the RBE variation regarding various target configurations; thus, survival measurements for Chinese hamster V 79 cells irradiated by graded dose of neutrons generated by a 43 MeV proton beam have been performed at 2 and 12 cm in water phantom with a thick beryllium target (T_t = 1.27 cm) followed by a hydrogeneous filter 4 cm thick or a thinner target (T_t = 0.79 cm); the two alternate methods give the same improvement in the neutron RBE which is then independent of depth, but the method of thinning the target is preferred because it is associated with a smaller reduction of dose rate. Further RBE estimations using filtration and transmission targets (SM82) improving dosimetry measurements should be undertaken.

CONCLUSIONS:

The data surveyed in this report show that the neutron beam produced by the Be+p reaction is promising in radiotherapy applications. Indeed, high neutron yields and suitable penetration depths can be achieved with protons of energies 40 MeV $\lesssim E_p \lesssim$ 70 MeV and targets of medium thicknesses supported by convenient backings to prevent heating problems and followed by hydrogeneous filters to reduce the undesirable low energy portion of the spectrum.

However, although the main shapes of the neutron spectra are well known for $E_p \leqslant 46$ MeV and $E_p \sim 100$ MeV, very scarce reliable data exist in the energy range 50 MeV $< E_p <$ 100 MeV, where, nevertheless, several dosimetric measurements are performed. Furthermore, the low energy part of the spectra is not yet well known because of the high thresholds varying from 0.3 MeV to 10 MeV, due to the limitations of the time-of-flight technique (e.g. neutron detector efficiency, proton beam bursts separation) used in most of the spectra measurements. This leads to uncertainties in absolute neutron yields and mean neutron energy values which have to be known with good accuracy for reliable dosimetric measurements. These quantities could be estimated from thin target data, as developed by Weaver et al. (WE73), but the existing $^{9}Be(p,n)^{9}B$ cross section measurements in the relevant energy range are too scanty (see Table 1).

Therefore, further experiments should be made to obtain lower neutron energy data by using either time-of-flight techniques in machines allowing longer separation periods of proton beam pulses or proton recoil spectrometry with suitable dE-E detector assemblies. Studies should also be undertaken to investigate the contribution of the low energy neutrons scattered by the beam collimator to the low energy tail of the spectra, as a function of the shape and composition of the collimators. Thin target measurements are, at last, required to complete the missing cross section data.

E_{th} - 3	CA76		Total neutron Yield: $N.\mu C^{-1}10^8$		
2.5 - 4.1	KE63			0 - 160	$\sigma(\theta)$: mb/sr
E_{th} - 5	GI59		σ_T: mb		
2.0 - 4.3	AL61			0 - 160	$\sigma(\theta)$: relative scale
2 - 5	MA56	0;90	$\sigma(\theta)$: mb/sr σ_T: mb		
2.3 - 5.4	MA59	0;45;90; 150	$\sigma(\theta,E_n)$: arbitrary scale		
		0;90	G.S. excitation curves, $\sigma(\theta)$: mb/sr		
5.5	CH78	15	N/Channel		
E_{th} - 5.8	MA55	≃ 0	$\sigma(\theta)$: mb/sr		
6.8	DR68	60	N/Channel	0 - 150	$\sigma(\theta)$: μb/sr
3 - 7	PO72		Total neutron Yield: $N.\mu C^{-1}10^9$		
8.1	WA65	30	N/Channel		
3.5 - 10.9	WA65			0 - 180	$\sigma(\theta)$: mb/sr
12	TO58	0	Neutron flux density: relative units Average neutron Energy: MeV		
12	LO81	0	Yield: N sr^{-1} s^{-1} A^{-1}		
8 - 14	SA60			0 - 150	$\sigma(\theta)$ G.S.: mb/sr
14.1	SA60	28;57	N/E_n	0 - 100	$\sigma(\theta)$ for four ^9B excited states neutron groups: mb/sr

TABLE 1

$^{9}Be(p,n)^{9}B$: Neutron Energy Spectra and Angular Distributions Measurements at $E_p \ll 120$ MeV

Abbreviations:

E_{th}: Proton Incident Threshold Energy = 2.044 MeV (Q = -1,850 MeV)
E_p: Proton Incident Energy
θ: Neutron Detection Angle
E_n: Neutron Energy
$\sigma(\theta,E_n) = d^2\sigma/d\Omega d\ E_n$: Differential Cross Section per unit neutron Energy range
$\sigma(\theta) = d\sigma/d\Omega$: Differential Cross Section
σ_T: Angle-Integrated Experimental Cross Section
G.S: ^{9}B Ground State
N: Number of detected neutrons

E_p(MeV)	References	Energy Spectra		Angular Distributions	
		θ (Degrees)	Measured Quantities : Units	θ Range (Degrees)	Measured Quantities: Units
$\simeq E_{th}$	TE64		σ_T: μb		
E_{th}	C070	0	Neutron Yield: relative scale		
$\simeq E_{th}$	SY70, SY71		σ_T: mb		

14.4	VE69		σ_T: mb/MeV		
14.8	KU73	0;15;30; 60;120;150	Yield: relative scale	0 - 150	Integrated yield: $N.sr^{-1}.\mu C^{-1}$
14.8	LO77*	20 0	Intensity: $N.sr^{-1}.s^{-1}.A^{-1}.MeV^{-1}$ Intensity: $N.sr^{-1}.s^{-1}.A^{-1}$. Average Energy for neutrons with E_n > 0.3 to 4.3 MeV: MeV		
15	MC75	0	$\sigma(\theta,E_n)$: $mb.sr^{-1}.MeV^{-1}$		
8 - 15.7	BY78; BY79; GO80			0 - 165	$\sigma(\theta)$ G.S.: mb/sr, $\sigma(\theta)$ for various ^9B excited states neutron groups: mb/sr
17.8	AR72	10 - 120	N/E_n		
18	VE69	0	$\sigma(\theta,E_n)$: $mb.sr^{-1}.MeV^{-1}$ $\sigma(\theta)$ for the neutrons with E_n > 3.3 MeV: mb/sr	0 - 170	$\sigma(\theta)$ for three different ΔE_n neutron groups: mb/sr
18	LO77*, LO81	0	Intensity: $N.sr^{-1}.s^{-1}.MeV^{-1}$ Average Energy for neutrons with E_n > 0.3 to 4.3 MeV: MeV Different target thicknesses	0 - 40	Intensity: 10^{16} $N.sr^{-1}.s^{-1}.A^{-1}$.
18.5	AN64			3 - 153	$\sigma(\theta)$: mb/sr
20	SL67	9;12;17	N/Channel		
20	AN70	15	N/E_n		
20	MC75	0	$\sigma(\theta,E_n)$: $mb.sr^{-1}.MeV^{-1}$		
22.5	HE77*	0	Yield: relative scale		
22.8	CA75			10 - 152	$\sigma(\theta)$: mb/sr

23	BE72, G080			12 - 156	$\sigma(\theta)$ for the G.S. and the 2.36 MeV state in ^{9}B neutron groups: mb/sr
23	L077*, L081	0	Intensity: $N.sr^{-1}.\ s^{-1}.\ A^{-1}.\ MeV^{-1}$ Average Energy for neutrons with $E_n > 0.3$ to 4.3 MeV: MeV. Different target thicknesses	0 - 40	Intensity: 10^{16} $N.sr^{-1}.\ s^{-1}.A^{-1}.$
25	J077*	0;10;20; 50	Yield: $N.\ C^{-1}.\ sr^{-1}.\ MeV^{-1}.\ 10^{15}$	0 - 50	Integrated Yield for neutrons with $E_n > 5$ MeV: $N.sr^{-1}.C^{-1}.10^{17}$
29.4	JU71, R076	0	$\sigma(\theta)$: mb/sr		
30	BA69	0	$\sigma(\theta,E_n)$: $mb.sr^{-1}.\ MeV^{-1}$		
30	CL70	30	$\sigma(\theta,E_n)$: $mb.sr^{-1}.\ MeV^{-1}$	0 - 60	$\sigma(\theta)$ for the G.S. and for three ^{9}B excited states neutron groups: mb/sr
30	J078*	0	Integrated Yield for neutrons with $E_n > 5$ MeV: $N.C^{-1}.sr^{-1}$ Yield: $N.C^{-1}.sr^{-1}.MeV^{-1}.10^{15}$ (unfiltered + filtered n beams). Average Neutron Energy: MeV		
35	AM77*	0	Yield. $N.sr^{-1}.{}_{\mu}C^{-1}.\ MeV^{-1}.10^{9}$ Integral Yield for neutrons with $E_n > 5.1$ MeV: $N_{\mu}C^{-1}.\ sr^{-1}$ Various target thicknesses		
35	HE77	0	Yield: relative scale		
35	J077*	0;5;15; 30;50	Yield: $N.sr^{-1}.C^{-1}.\ MeV^{-1}.\ 10^{15}$	0 - 50	Integrated Yield for neutrons with $E_n > 5$ MeV: $N.sr^{-1}.C^{-1}.10^{17}$

50	CL70	30	$\sigma(\theta,E_n)$: mb.sr^{-1}.MeV^{-1}	0 - 60	$\sigma(\theta)$ for the G.S. and for the 2.3 MeV excited state in ^{9}3 neutron groups: mb/sr
50	B078	20	$\sigma(\theta,E_n)$: mb.sr^{-1}.MeV^{-1}		
50.6	JU71, R076	0	$\sigma(\theta)$: mb/sr		
55	J077*	0;5;15; 30; 50	Yield: N.C^{-1}.sr^{-1}.MeV^{-1}.10^{15}	0 - 50	Integrated Yield for neutrons with E_n > 5 MeV; N.C^{-1}.sr^{-1}.MeV^{-1}.10^{17}
65.4	AM77*	0	Yield: N.sr^{-1}.MeV^{-1}.μC^{-1}.10^{9} Integral: Yield for neutrons with E_n > 9.1 MeV: N.sr^{-1}.μC^{-1} various target thicknesses		
65.5	HE77*	0	Yield: relative scale		
90	HA80		Yield: N/MeV Average neutron Energy: MeV (unfiltered + filtered neutron beams)		
100.2	MA77	0	Yield: relative scale		
101	HA78*		Yield: N/MeV Average neutron Energy: MeV (unfiltered + filtered neutron beams)		
120	G080			1 - 22	$\sigma(\theta)$ for the G.S. and for the 2.6 MeV excited state in ^{9}B neutron groups: mb/sr

* works already reported in Cross' survey (CR78)
** works announced in Cross' survey but published later

35	WA79**	0;15;45	Yield: $N.MeV^{-1}.sr^{-1}.\mu C^{-1}$. Integral Yield for neutrons with $E_n > 5$ MeV and total integral Yield: $N.sr^{-1}.\mu C^{-1}.10^9$		
35	UL81	0	Yield: $N.MeV^{-1}.sr^{-1}.\mu C^{-1}.10^9$		
39	TU80	0	Yield: Relative Units		
39.2	JU71, RO76	0	$\sigma(\theta,E_n)$: $mb.sr^{-1}.MeV^{-1}$ $\sigma(\theta)$: mb/sr		
40	JO78*	0	Yield: $N.C^{-1}.sr^{-1}.MeV^{-1}.10^5$ Integrated Yield for neutron with $E_n > 5$ MeV: $N.C^{-1}.sr^{-1}$. Average Neutron Energy: MeV (unfiltered + filtered n beams)		
41 - 42	WE78, GR79**	0	Yield: $N.sr^{-1}.MeV^{-1}.nC^{-1}.10^4$ Integral Yield: $N.sr^{-1}.nC^{-1}.10^8$ Average Neutron Energy: MeV (filtered neutron beams)		
43	RO81b, HA82		Integrated Yield: N/MeV (unfiltered + filtered neutron beams)		
45	HE77*	0	Yield: relative scale		
45	JO77*	0;5;15; 30;50	Yield: $N.C^{-1}.sr^{-1}.MeV^{-1}.10^{15}$	0 - 50	Integrated Yield for neutrons with $E_n > 5$ MeV: $N.sr^{-1}.C^{-1}.10^{17}$
46	WA79**	0;15;45	Yield: $N.MeV^{-1}.sr^{-1}.\mu C^{-1}$ Integral Yield for neutrons with $E_n >$ 5 MeV and total Integral Yield: $N.sr^{-1}\mu C^{-1}.10^9$		
50	BA69	0	$\sigma(\theta,E_n)$: $mb.sr^{-1}.MeV^{-1}$		

TABLE 2

p + Be neutrons integral yields and average energies at different proton energies

E_p (MeV)	References	T. thickness (cm)	Filtration (cm)	Cut-off Energy (MeV)	0° Integral Yield 10^{10} n/sr/μC	Average Energy (MeV)
12	L081	0.11	-	0.4	0.8	2.2
18	L081	0.23	-	0.4	1.8	3.7
		0.12	-	0.4	1.0	4.8
23	L081	0.13	-	0.4	1.1	7.6
		0.25	-	0.4	2.0	6.2
		0.36	-	0.4	2.8	5.1
25	J077	0.46	0.3 (Al)	5	0.8	9.9*
35	WA79	1.43	-	0	4.44 ± 0.26	
		1.43	-	5	3.06 ± 0.18	19.3
35	UL81	1.16	-	1	1.66	
40	J078	1.27	-	5	3.2 ± 0.6	17.6
		1.27	5.82 (CH_2)	5	2.1 ± 0.4	18.5
41	GR79	1.22	0.41 (Al)	1.9	5.15	17.1
		1.22	0.41 (Al)	4.1	4.39	19.6
		1.22	0.41 (Al) + 6 (CH_2)	1.9	2.45	20.4
		1.22	0.41 (Al) + 6 (CH_2)	4.1	2.30	21.5
46	WA79	1.43	-	0	9.04 ± 0.81	-
		1.43	-	5	7.02 ± 0.63	24.9

E_p (MeV)	References	T. thickness (cm)	Filtration (cm)	Cut-off Energy (MeV)	0^o Integral Yield 10^{10} n/sr/μC	Average Energy (MeV)
65	AM77	2.41	-	9.1	8.8	
		1.60	-	9.1	7.0	
66	HA76					22
90	HA80	3.0	0.25 (Ta) + 1.0 (Al)	10		42
		3.0	0.25 (Ta) + 1.0 (Al) + 10 (CH_2)	10		44.6
101	HA80	4.25	1.3 (Al)	10	26**	47.5
		4.25	1.3 (Al) + 10 (CH_2)	10		51.4

* Average Energy for neutrons with E_n>0 MeV
** This yield refers to all neutron energies, as estimated by use of fluence to dose factors (HA77)

Figure Captions

Figure 1

Angular distributions of some neutron groups from the proton bombardement of thin beryllium targets measured by different authors at different proton energies E_p.

Figure 2

Angular distributions of integrated neutron yields from the proton bombardement of thick beryllium targets measured by different authors at different proton energies and with different neutron thresholds.

Figure 3

0^o neutron spectra from protons on thick beryllium measured by different authors at 23 MeV $\leqslant E_p \leqslant$ 46 MeV. For each curve, the target thickness T_t is reported.

Figure 4

0^o neutron spectra from proton on thick beryllium targets measured by different authors at E_p = 65 MeV and $E_p \simeq$ 100 MeV. For each curve, the target thickness T_t is reported.

Figure 5

Comparison of the 0^o neutron spectra obtained from 42 MeV protons on a thick beryllium target without filter and with a 6 cm polyethylene filter.

Figure 6

Depth at 50%of maximum total dose measured in water at 125 cm TSD as a function of proton energy and filter thickness, from (BE80).

Figure 7

Variation of the dose rate as a function of depth of 50% of maximum dose for 5 cm and 6 cm filtration and various beryllium target thicknesses removing the energy e_t from the $E_p \simeq$ 41 MeV proton beam as measured by Rosenberg et al. (RO81a: e_t = 41.3 MeV; 22.8 MeV; 15.4 MeV and 8.2 MeV corresponding respectively to the points A, B, C, and D) and by Smathers et al. (SM82: e_t = 41 MeV; 25 MeV and 15 MeV corresponding respectively to the points G, F and E.)

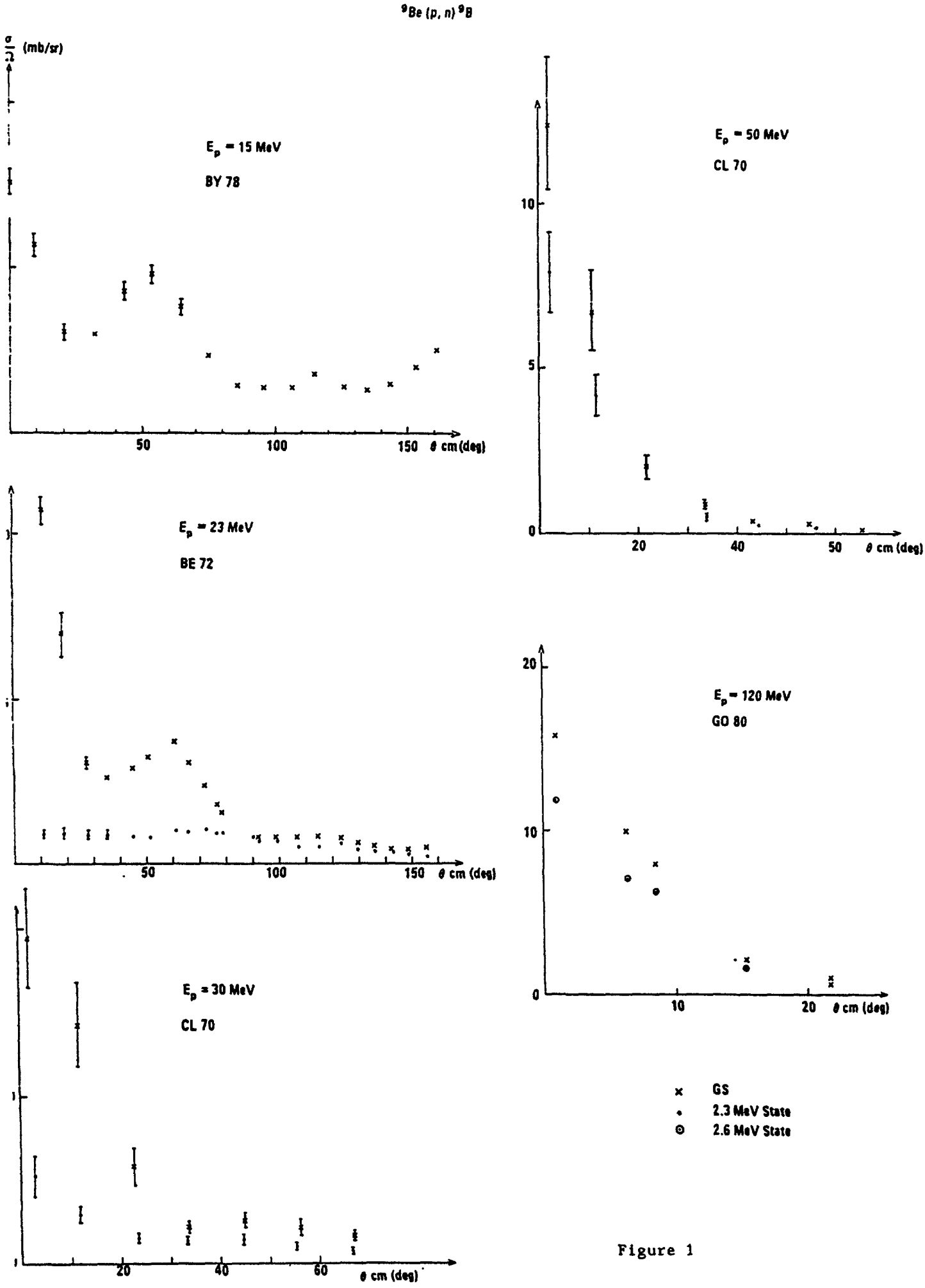
$^{9}Be\ (p, n)\ ^{9}B$
$\frac{d\sigma}{d\Omega}$ (mb/sr)
E_p = 15 MeV
BY 78
50
100
150
θ cm (deg)
E_p = 50 MeV
CL 70
10
5
0
20
40
50
θ cm (deg)
E_p = 23 MeV
BE 72
50
100
150
θ cm (deg)
20
E_p = 120 MeV
GO 80
10
0
10
20
θ cm (deg)
E_p = 30 MeV
CL 70
20
40
60
θ cm (deg)
GS
2.3 MeV State
2.6 MeV State

Figure 1

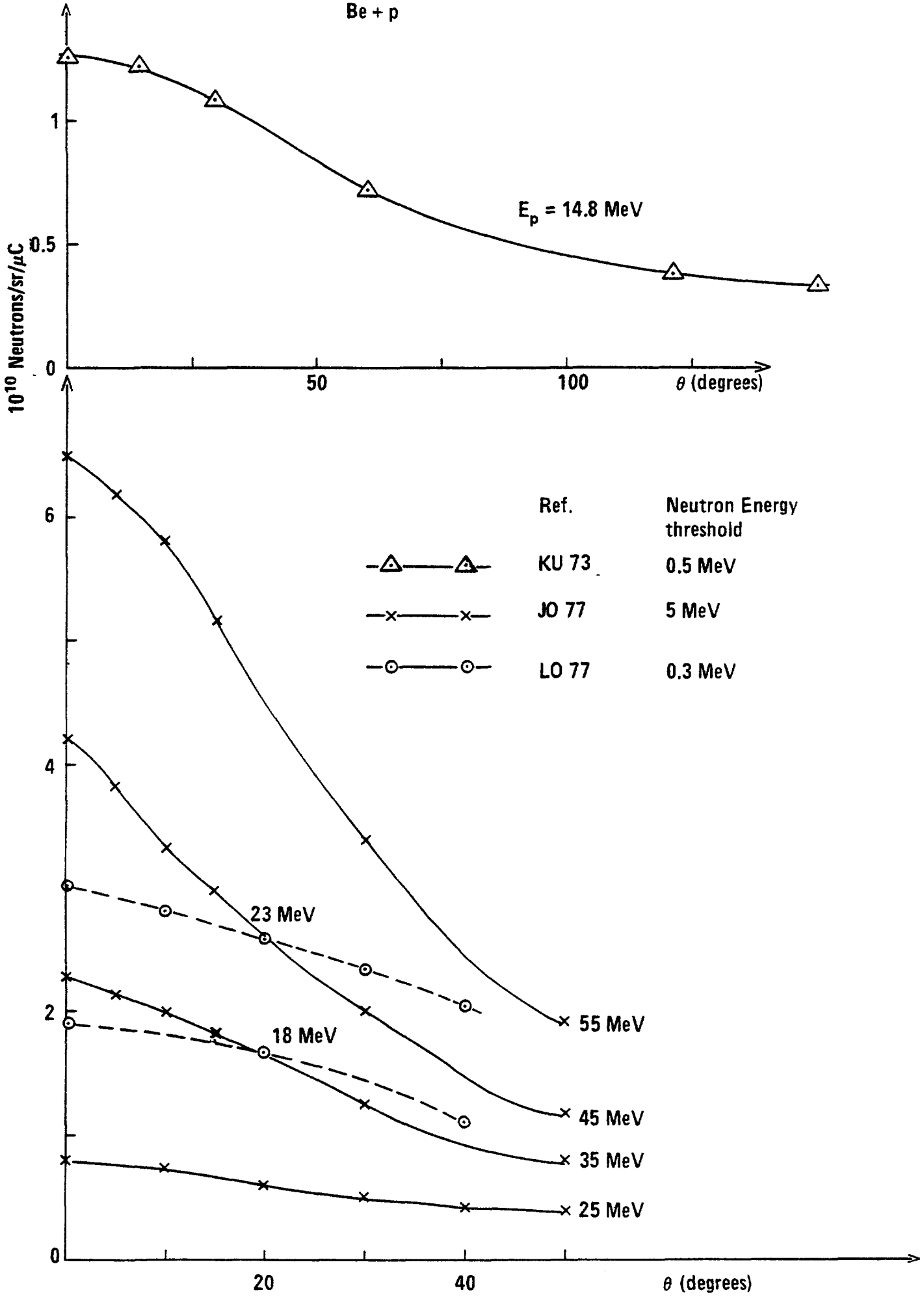
Be + p
E_p = 14.8 MeV
10^{10} Neutrons/sr/μC
θ (degrees)
Ref.
Neutron Energy threshold
KU 73
0.5 MeV
JO 77
5 MeV
LO 77
0.3 MeV
23 MeV
18 MeV
55 MeV
45 MeV
35 MeV
25 MeV
θ (degrees)

Figure 2

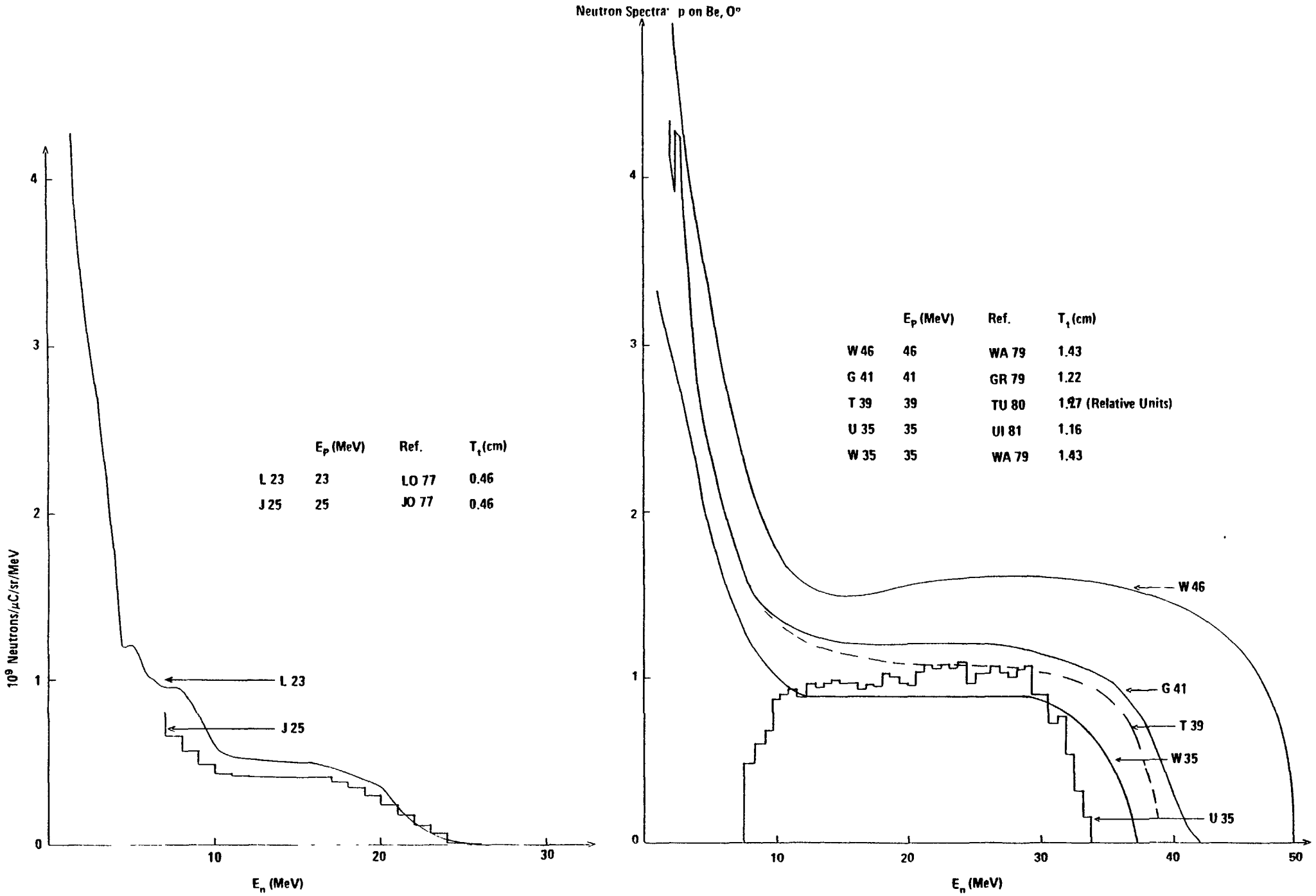
Neutron Spectra p on Be, 0°
10^9 Neutrons/μC/sr/MeV
E_n (MeV)
E_p (MeV) Ref. T_t(cm)
L 23 23 LO 77 0.46
J 25 25 JO 77 0.46
L 23
J 25
E_p (MeV) Ref. T_t(cm)
W 46 46 WA 79 1.43
G 41 41 GR 79 1.22
T 39 39 TU 80 1.27 (Relative Units)
U 35 35 UI 81 1.16
W 35 35 WA 79 1.43
W 46
G 41
T 39
W 35
U 35

Figure 3

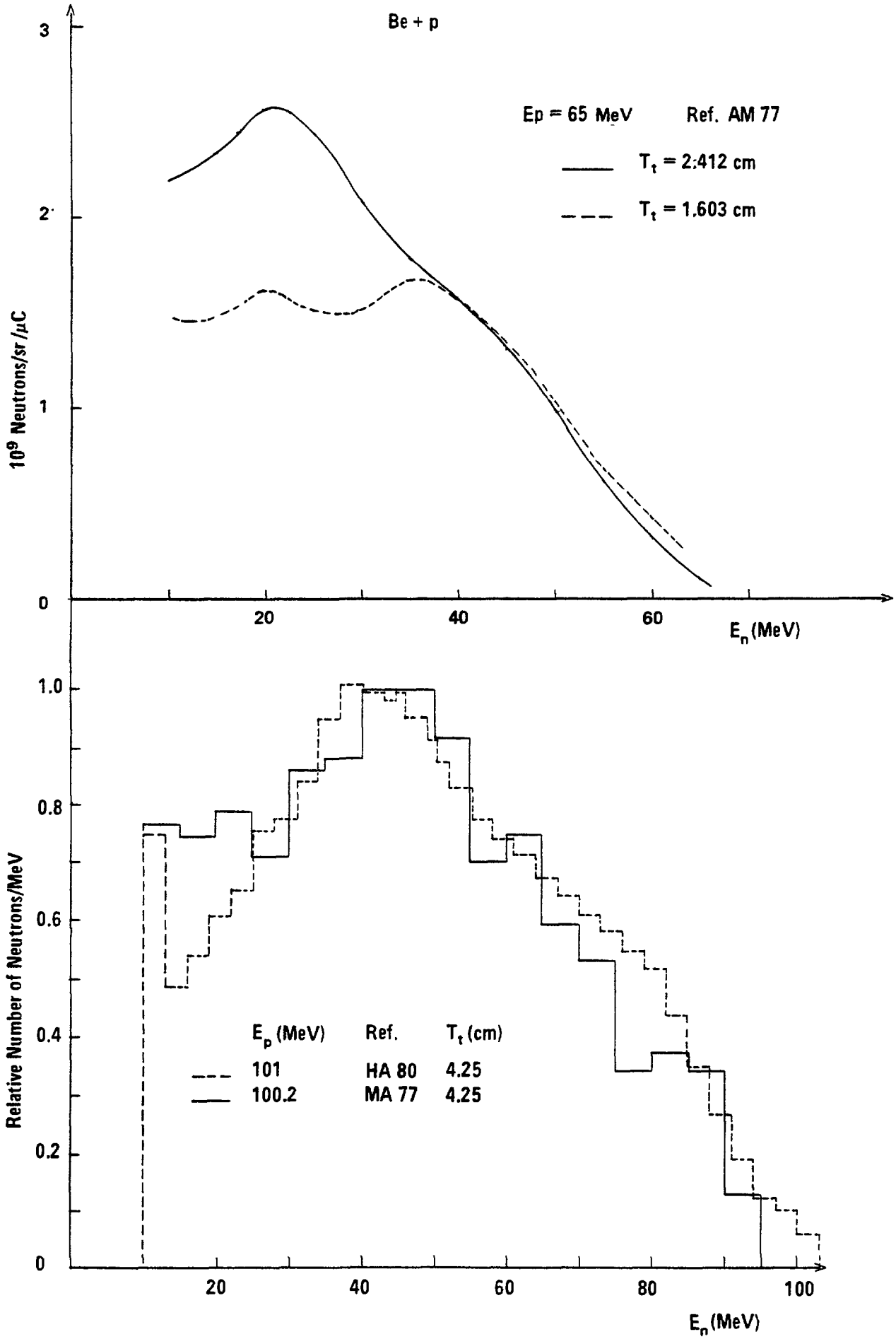
Be + p
Ep = 65 MeV
Ref. AM 77
T_t = 2:412 cm
T_t = 1.603 cm
10^9 Neutrons/sr/μC
E_n (MeV)
Relative Number of Neutrons/MeV
E_p (MeV)
Ref.
T_t (cm)
101
HA 80
4.25
100.2
MA 77
4.25
E_n (MeV)

Figure 4

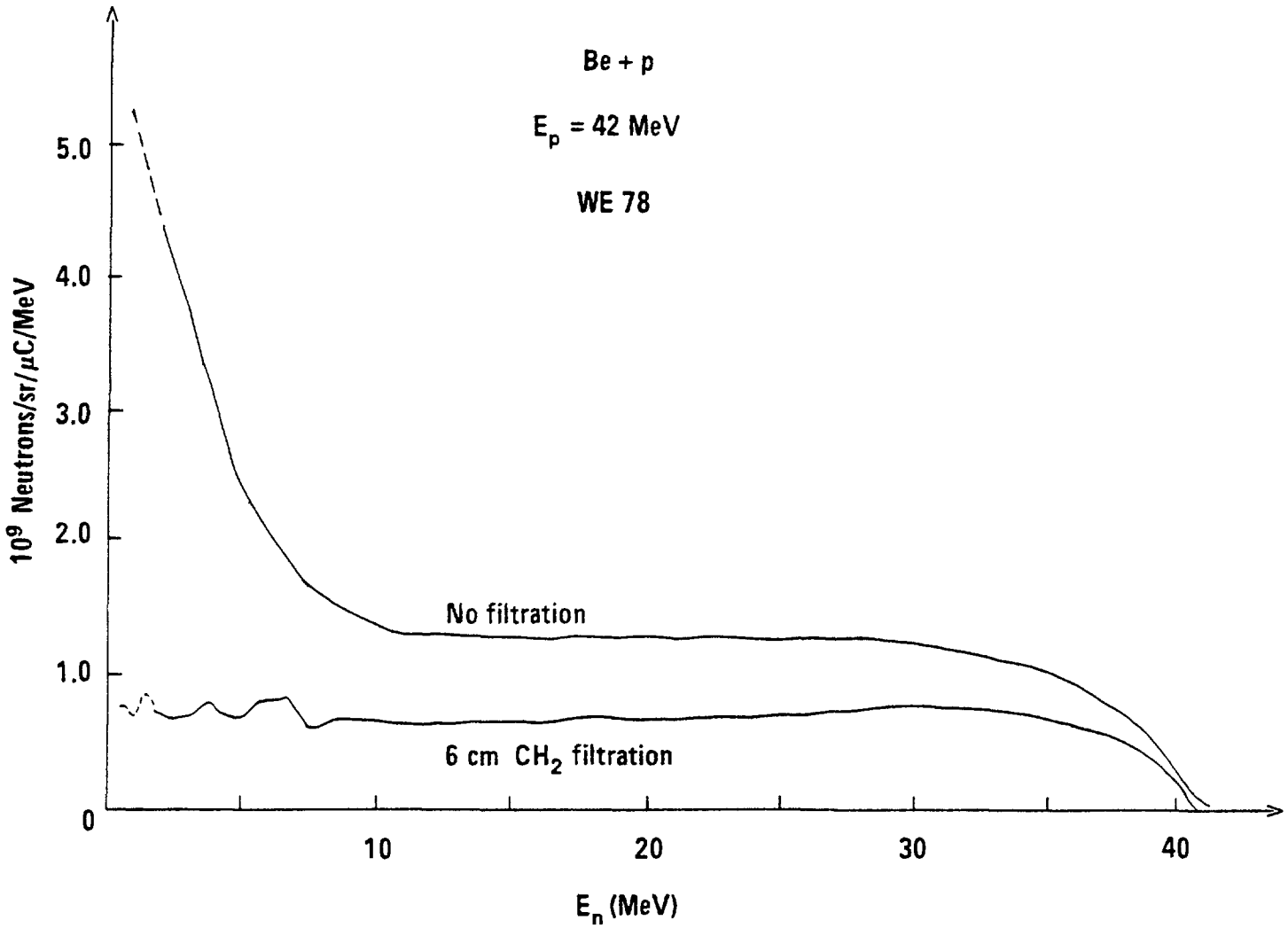
Be + p
E_p = 42 MeV
WE 78
5.0
4.0
3.0
2.0
1.0
0
10^9 Neutrons/sr/μC/MeV
No filtration
6 cm CH_2 filtration
10
20
30
40
E_n (MeV)

Figure 5

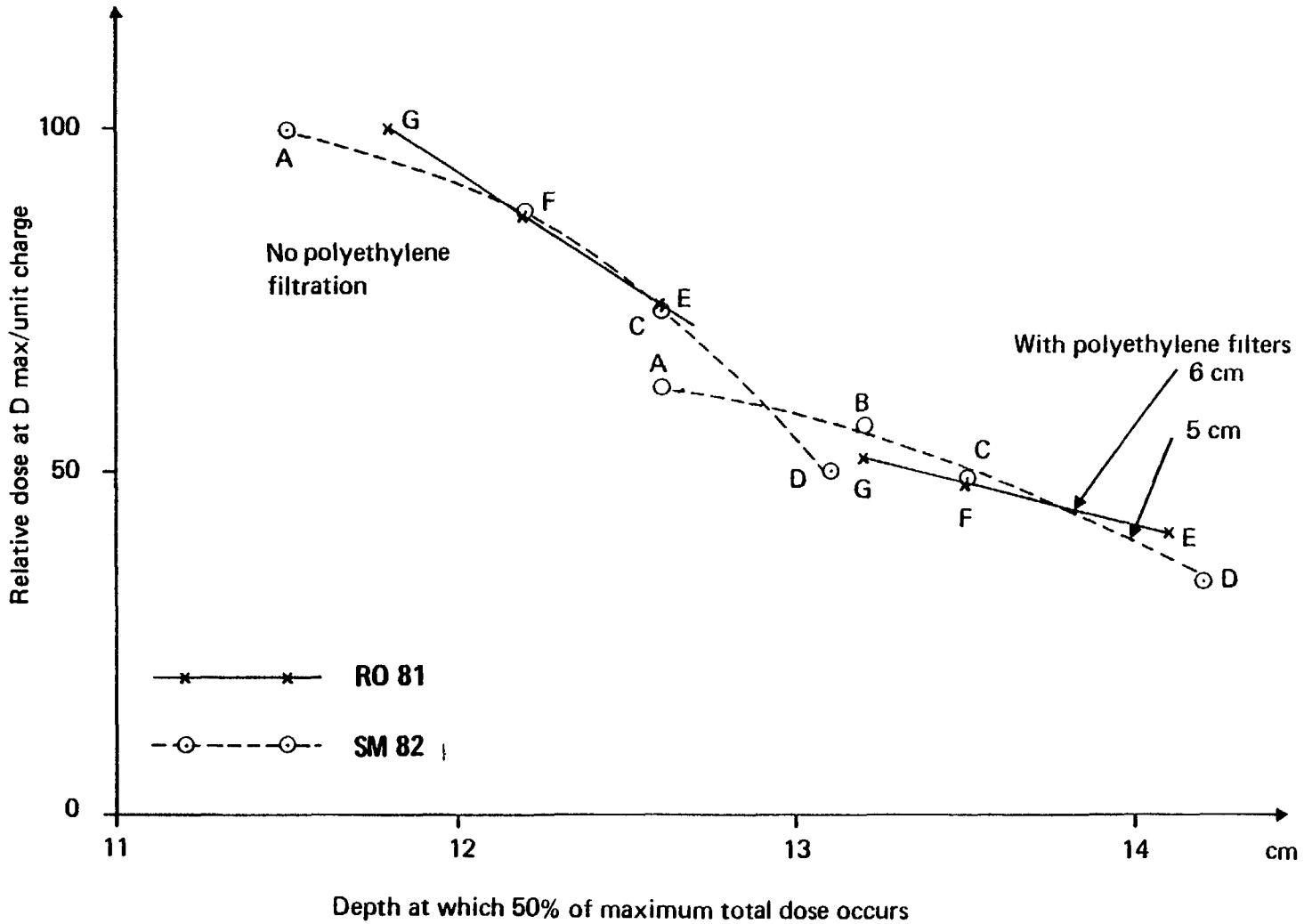
100
50
0
Relative dose at D max/unit charge
No polyethylene
filtration
With polyethylene filters
6 cm
5 cm
A
G
F
E
C
A
B
C
D
G
F
E
D
RO 81
SM 82
11
12
13
14
cm
Depth at which 50% of maximum total dose occurs

Fig.7

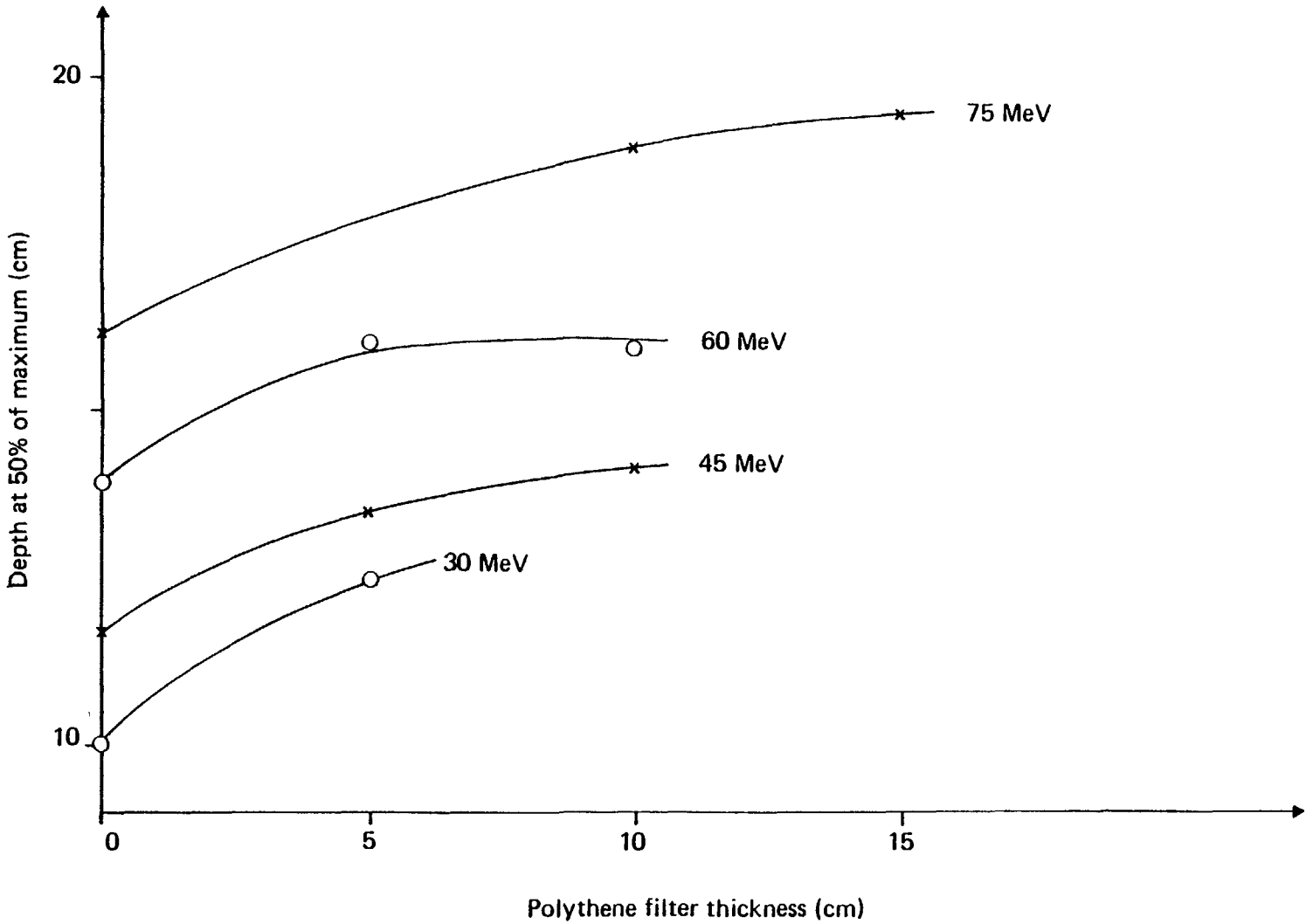
20
10
Depth at 50% of maximum (cm)
75 MeV
60 MeV
45 MeV
30 MeV
0
5
10
15
Polythene filter thickness (cm)

Fig.6

REFERENCES

MA55: J.B. MARION, T.W. BONNER and C.F. COOK, Phys. Rev. 100 (1955) 91

MA56: J.B. MARION, Phys. Rev. 103 (1956) 713

TO58: E. TOCHILIN and G.D. KOHLER, Health Phys. 1 (1958) 332

GI59: J.H. GIBBONS and R.L. MACKLIN, Phys. Rev. 114 (1959) 571

MA59: J.B. MARION and J.S. LEVIN, Phys. Rev. 115 (1959) 144

SA60: Y. SAJI, J. Phys. Soc. Japan 15 (1960) 367

AL61: R.D. ALBERT, S.D. BLOOM and N.K. GLENDENNING ,Phys. Rev. 122 (1961) 862

KE63: C.A. KELSEY, G.P. LIETZ, S.F. TREVINO and S.E. DARDEN, Phys. Rev. 129 (1963) 759

AN64: J.D. ANDERSON, C. WONG, J.W. McCLURE and B.D. WALKER, Phys. Rev. 136 (1964) B 118

TE64: E. TERANISHI and B. FURUBAYASHI, Phys. Lett. 9 (1964) 157

WA65: B.D. WALKER, C. WONG, J.D. ANDERSON and J.W. McCLURE, Phys. Rev. 137 (1965) B 1504

SL67: R.J. SLOBODRIAN, H. BICHSEL, J.S.C. McKEE and W.F. TIVOL, Phys. Rev. Lett. 19 (1967) 595

DR68: I.P. DRYAPACHENKO, V.A. KORNILOV, O.F. NEMETZ and V.A. PILIPCHENKO, Sov. J. Nucl. Phys. 6 (1968) 321

BA69: C.J. BATTY, B.E. BONNER, A.I. KILVINGTON, C. TSCHÅLAER and L.E. WILLIAMS, Nucl. Instrum. Methods 68 (1969) 273

VE69: V.V. VERBINSKI and W.R. BURRUS, Phys. Rev. 177 (1969) 1671

AN70: J.D. ANDERSON, C. WONG, B.A. POHL and J.W. McCLURE, Phys. Rev. C. 2 (1970) 319

CL70: A.S. CLOUGH, C.J. BATTY, B.E. BONNER and L.E. WILLIAMS, Nucl. Phys. A 143 (1970) 385

CO70: M.D. COOPER, A.S. FIGUERA, G. PFEUFER and G. RANDERS-PEHRSON, Nucl. Phys. A 142 (1970) 445

SI70: V.S. SISKIN, V.N. DOMORATSKII, L.V. DONETSKOV, A.N. VORONIN, M.M. NOVIKOV, A.N. KUDRYAVTSEV, G.D. BATYSHEV and V.F. TSESHKOVSKAYA, Sov. J. Nucl. Phys. 10 (1970) 643

JU71: J.A. JUNGERMAN, F.P. BRADY, W.J. KNOX, T. MONTGOMERY, M.R. McGIE, J.L. ROMERO and Y. ISHIZAKI, Nucl. Instrum. Methods 94 (1971) 421

SI71: V.S. SISKIN, V.N. DOMORATSKII, L.V. DONETSKOV, A.N. VORONIN, M.M. NOVIKOV, A.N. KUDRYAVTSEV, G.D. BATYSHEV, S.K. BARVIN and V.F. TSESHKOVSKAYA, Sov. J. Nucl. Phys. 12 (1971) 9

AR72: U.R. ARIFKHANOV, M. GULYAMOV, B.I. ISLAMOV and E. ERGASHOV, Sov. J. Nucl. Phys. 15 (1972) 610

BE72: R.D. BENTLEY, Ph.D. Thesis, University of Colorado, Dpt. of Phys. and Astrophys., (1972)

PO72: K. PORGES, J.L. SNELGROVE, R. GOLD, A. DEVOLPI, R.J. ARMANI and C.E. COHN, Rep. ANL - 7910 (1972) 361

KU73: F.T. KUCHNIR, L.S. SKAGGS, A.J. ELWYN AND F.P. MOORING, Rep. USNDC3 (1973) 8

WE73: K.A. WEAVER, J.D. ANDERSON, H.H. BARSCHALL and J.C. DAVIS, Nucl. Sc. Engineering, 52 (1973) 35

CA75: J.D. CARLSON, C.D. ZAFIRATOS and D.A. LIND, Nucl. Phys. Nucl. Phys. A 249 (1975) 29

MC75: M.W. MCNAUGHTON, N.S.P. KING, F.P. BRADY, J.L. ROMERO and T.S SUBRAMANIAN, Nucl. Instrum. Methods 130 (1975) 555

CA76: J. CAMPBELL and MALCOLM C. SCOTT, Proc. 4th Conf. on the use of small accelerators, Denton, TX. USA. Conf. 761059 (Oct. 1976) 517

HA76: G.H. HARRISSON, E.B. KUBICZECK and J.E. ROBINSON, Br. J. Radiol. 49 (1976) 733

RO76: J.L. ROMERO, F.P. BRADY and J.A. JUNGERMAN, Nucl. Instrum. Methods 134 (1976) 537

AM77: H.I. AMOLS, J.F. DICELLO, M. AWSCHALOM, L. COULSON, S.W. JOHNSEN and R.B. THEUS, Med. Phys. 4 (1977) 486

CR77: W.G. CROSS, "Nuclear Data Reguirements for radiotherapy with neutrons" INDC(CAN)-17/G (1977)

HA77: G.H. HARRISSON, C.R. COX, E.B. KUBICZEK and J.E. ROBINSON, Rep. NBSIR 77-1279 (1977) 19

HE77: P.H. HEINTZ, S.W. JOHNSON and N.F. PEEK, Med. Phys. 4 (1977) 250

JO77: S.W. JOHNSEN, Med. Phys. 4 (1977) 255

LO77: M.A. LONE, C.B. BIGHAM, J.S. FRASER, H.R. SCHNEIDER, T.K. ALEXANDER, A.J. FERGUSON and A.B. McDONALD, Nucl. Instrum. Methods 143 (1977) 331

MA77: R. MADEY, F.M. WATERMAN and A.R. BALDWIN, Med. Phys. 4 (1977) 322

BO78: M. BOSMAN, P. LELEUX, P. LIPNIK, P. MACQ, J.P. MEULDERS, R. PETIT, C. PIRART and G. VALENDUC, Nucl. Instrum. Methods 148 (1978) 363

BY78: R.C. BYRD, K. MURPHY, P. GUSS, C. FLOYD and R.L. WALTER, TUNL Annual Report OR 1667-17 (1978) XVII-20
R.C. BYRD, Ph. D. Thesis, University of Colorado, Dept. of Phys. (1978)

CH78: J.C. CHOU, C.M. FOU, C.S. LIN, P.S. SONG, M. WEN and Y.C. LIU, J. Phys. Soc. Japan 44 (1978) 1

CR78: W.G. CROSS, "Nuclear Data for Radiotherapy with Neutrons". Proc. Int. Conf. on Neutron Physics and Nuclear Data for Reactors and other Applied Purposes, Harwell - U.K., (25-29 Sept. 1978) p. 648-666

GR78: W.H. GRANT, P.R. ALMOND, and V.A. OTTE, Proc. 3rd Symp. on Neutron dosimetry in Biol. and Med. Rep. EUR. 5848 DE/EN/FR (1978) 303

HA78: G.H. HARRISSON, C.R. COX, E.B. KUBICZEK and J.E. ROBINSON, Proc. third symposium on Neutron Dosimetry in Biology and Medecine, Neuherberg, G. BURGER and H.G. HEBERT, Eds., Rep. EUR 5848 DE/EN/FR (1978) 471

JO78: S.W. JOHNSEN, Phys. Med. Biol. 23 (1978) 499

MI78: B.J. MIJNHEER, J. ZOETELIEF and J.J. BROERSE, Br. J. Radiol. 51 (1978) 122

WE78: A.H. WELLS, Thesis, Los Alamos scient. Lab., Univ. of California, Rep. LA-7288 -T (1978)

AL79: P.R. ALMOND, V.A. OTTE, W.H. GRANT, J. SMATHERS and R. GRAVES, I.E.E.E. Trans. Nucl. Sc. NS-26, No. 1 (1979) 1724

BY79: R.C. BYRD, C.E. FLOYD, R.K. MURPHY, P.P. GUSS and R.L. WALTER, Rep. TUNL XVIII, DOE./TIC 11133 (1979) 32

GR79: R.G. GRAVES, J.B. SMATHERS, P.R. ALMOND, W.H. GRANT and V.A. OTTE, Med. Phys. 6 (1979) 123

WA79: F.M. WATERMAN, F.T. KUCHNIR, L.S. SKAGGS, R.T. KOUZES and W.H. MOORE, Med. Phys. 6 (1979) 160 and Med. Phys. 6 (1979) 432

AW80: M. AWSCHALOM, I. ROSENBERG, R. TEN HAKEN, L. COHEN and F.R. HENDRICKSON, Treatment planning for external beam therapy with neutrons, ISBN 3-541-70271-0 (18-19 Sept. 1980) G. BURGER, Ed..

AW80a: M. AWSCHALOM and I. ROSENBERG, Med. Phys. 7 (1980) 492

AW80b: M. AWSCHALOM, I. ROSENBERG, T.Y. KUO and J.L. TOM, Med. Phys. 7 (1980) 495

BE80: D.K. BEWLEY, J.P. MEULDERS, M. OCTAVE-PRIGNOT and B.C. PAGE, Phys. Med. Biol. 25 (1980) 887

GO80: C.D. GOODMAN, The (p,n) Reactions and the Nucleon-Nucleon force - Plenum Publishing Corporation, New York (1980) 149

HA80: G.H. HARRISSON, E. K. BALCER-KUBICZEK and C.R. COX, Med. Phys. 7 (1980) 348

MA80: E.P. MALAISE, M. GUICHARD, J. GUEULETTE, M. OCTAVE PRIGNOT and A. WAMBERSIE, Int. J. Radiat. Biol. 38 (1980) 110

TU80: R.F. TURCO, R. GAHBAUER, A. RODRIGUEZ-ANTUNEZ, J.L. HORTON, W.K. ROBERTS and J.W. BLUE, Treatment planning for external beam therapy with neutrons - ISBN.3-541-70271-0 - Muenchen Germany - (Sept. 1980). G. BURGER Ed.

AW81: M. AWSCHALOM and I. ROSENBERG, Med. Phys. 8 (1981) 105

BR81: J.J. BROERSE and J.J. BATTERMANN, Med. Phys. 8 (1981) 751

LO81: M.A. LONE, A.J. FERGUSON and B.C. ROBERTSON, Nucl. Instrum. Methods 189 (1981) 515

RO81: I. ROSENBERG and M. AWSCHALOM, Med. Phys. 8 (1981) 99

RO81a: I. ROSENBERG, M. AWSCHALOM, T.Y. KUO and J.L. TOM, Med. Phys. 8 (1981) 808

RO81b: W.K. ROBERTS, J. BLUE, Neutron yields and spectra from 43 MeV protons on thick and thin Be targets. Works in Progress Paper 544. Annual Meeting of the Radiolobical Society of North America (1981).

UL81: J.L. ULLMANN, N. PEEK, S.W. JOHNSEN, A. RAVENTOS and P. HEINTZ, Med. Phys. 8 (1981) 396

VA81: J. VAN DAM and A. WAMBERSIE, Br. J. Radiol. 54 (1981) 921.

AW82: M. AWSCHALOM, I. ROSENBERG and R.K. TEN HAKEN, Med. Phys. 9 (1982) 884

BR82: N. BRETEAU, R. SABATIER, J.C. BAJARD and J. GUEULETTE, Ninth Int. Conf. on Cyclotrons and their Applications. Caen, France (7-10 Sept. 1981). Les Ulis (France) - les Editions de la Physique (1982) p. 703.

HA82: E.J. HALL, M. ZAIDER, R. BIRD, M. ASTOR and W. ROBERTS, Br. J. Radiol. 55 (1982) 640

HA82a: E.J. HALL, Rep. DOE/EV/04733-5* (1982) p. 114

SM82: J.B. SMATHERS, R.G. GRAVES, L. EARLS, V.A. OTTE and P.R. ALMOND, Med. Phys. 9 (1982) 856

TO82: J.L. TOM, T.Y.T. KUO and G.O. HENDRY, Ninth Int. Conf. on Cyclotrons and their Applications. Caen, France (7-10 Sept. 1981). Les Ulis (France) - les Editions de la Physique (1982) p. 707.

AW83: M. AWSCHALOM, I. ROSENBERG and A. MRAVCA, Med. Phys. 10 (1983) 395 and M. AWSCHALOM, I. ROSENBERG and R.K. TEN HAKEN, Med. Phys. 10 (1983) 436

HA83: E.J. HALL, M. ZAIDER and R. BIRD, Br. J. Radiol. 56 (1983) 349

ME83: J.P. MEULDERS, S. VYNCKIER, P. PIHET and A. WAMBERSIE, Nuclear Data for Science and Technology, K.H. BvCKHOFF, Ed. (1983), ECSC, EEC, EAEC, Brussels and Luxembourg.

TE83: R.K. TEN HAKEN, M. AWSCHALOM and I. ROSENBERG, Health Phys. 44 (1983) 277

VY83: S. VYNCKIER, P. PIHET, J.M. FLEMAL, J.P. MEULDERS AND A. WAMBERSIE, Phys. Med. Biol. 28 (1983) 685.